ELSEVIER

Journal of Chromatography A, 773 (1997) 33–51

JOURNAL OF CHROMATOGRAPHY A

Study of the physico-chemical properties of some packing materials III. Pore size and surface area distribution

Hong Guan-Sajonz[a,b], Georges Guiochon[a,b,*], Evelyn Davis[c], Kim Gulakowski[c], David W. Smith[c]

[a]*Department of Chemistry, The University of Tennessee, Knoxville, TN 37996-1600, USA*
[b]*Chemical and Analytical Sciences Division, Oak Ridge National Laboratory, Oak Ridge, TN 37831-6120, USA*
[c]*Micromeritics, Norcross, GA 30093-1877, USA*

Received 26 August 1996; revised 31 January 1997; accepted 10 February 1997

Abstract

The pore structures of four conventional stationary phases for reversed-phase liquid chromatography have been studied and compared. Helium pycnometry was used to determine the total porosity of the packing. Nitrogen sorptometry, inverse size-exclusion chromatography and mercury intrusion porosimetry have been applied to Kromasil, Vydac, YMC and Zorbax 10 μm particles of C_{18} chemically bonded silica. The agreement between the results derived from the three methods used for the determination of the volume pore size and the surface area distributions is excellent.

Keywords: Stationary phases, LC; Pore size distribution; Surface area distribution

1. Introduction

The physico-chemical properties of the stationary phases used in liquid chromatography are critical for the achievement of high-performance in chromatography and specially of high column efficiency [1]. The pore size distribution and the pore connectivity have been recognized as the key properties controlling the mass transfer across the particles, hence the column efficiency [2]. Still, in spite of considerable work undergone on the study of the performance of stationary phases used in high-performance preparative liquid chromatography, little is known regarding such fundamental properties as the pore size distribution of commercial stationary phases.

Mercury intrusion porosimetry [3] and nitrogen sorptometry [4,5] are the most common methods used for the determination of pore size distributions. Mercury intrusion porosimetry is based on the inverse relationship between the pressure needed to force intrusion of mercury inside a pore and the dimension of the pore opening [3]. The use of this method requires the knowledge of the wetting angle of the surface by mercury. Because mercury has a very high energy surface and an extremely high surface tension, it poorly wets most surfaces. However, the accurate determination of the pore size distribution requires a corresponding accuracy in the estimate of this angle which can vary slightly with the chemical nature of the surface. Nitrogen sorptometry is based on the quantitative interpretation

*Corresponding author. Corresponding address: Department of Chemistry, The University of Tennessee, Knoxville, TN 37996-1600, USA.

PII S0021-9673(97)00201-X

of the adsorption and desorption isotherms of nitrogen and of the adsorption hysteresis or difference between these two experimental isotherms [4,5].

While these two methods require dedicated instruments and proper skills in the interpretation of the results obtained, chromatographers have long been tempted with the use of inverse size-exclusion chromatography to achieve the same purpose [6–8]. Size-exclusion chromatography (SEC) separates the molecules contained in a sample, based on the differences between their molecular size (in principle their molecular volume, but the latter is strongly correlated with the molecular mass, easier to determine) [8]. Inverse size-exclusion chromatography (ISEC) aims at determining the pore size distribution of a sample of porous particles. This method is based on a relationship between the retention volumes of samples of polymeric fractions of known molecular masses and this mass [9]. Halasz and Martin [7] have developed from it a simple correlation between SEC data for polystyrene samples of known molecular mass and low polydispersity. Knox and Scott [8] have developed a more sophisticated model and shown agreement between the pore size distributions derived by ISEC and by mercury intrusion porosimetry. The empirical model of Halasz and Martin has not been so tested yet. Nevertheless, results obtained with it have been consistent and useful [7,10–12].

As part of our study of the performance of various packing materials for preparative liquid chromatography, we have determined the pore size distribution of four different C_{18} bonded silica-based stationary phases commonly used, Kromasil, Vydac, YMC and Zorbax. Results have been obtained using the three methods described above. Their comparison indicates the limits of ISEC compared to the other two procedures. These results should be completed by the determination of the pore connectivity which is in progress and will be reported later.

2. Theory

2.1. Helium pycnometry

The solid volume fraction of all samples was determined by helium pycnometry. A known mass of the material is placed in a cylinder of known volume which is flushed with helium and closed. The pressure inside the cylinder is adjusted to a predetermined value and its exact value is noted. A second, similar cylinder of known volume is filled with helium, under a different, known pressure. A valve is then opened between these two cylinders and the new pressure is noted. The ratio between these two pressures is directly related to the volume occupied by the solid material in the sample (including the non-connected pore volume in the particles, if any). This provides the apparent density of the particle skeleton and their specific unaccessible volume.

2.2. Mercury intrusion porosimetry

A known mass of sample is placed in an appropriate container [3]. To allow mercury to penetrate all pores without other impediments than the one resulting from its contact angle, the sample is evacuated prior to any measurement. Then, mercury is pushed into the chamber under a known pressure and the volume of mercury entering the chamber is noted. After equilibrium has been reached, the pressure is increased by successive increments, following an exponential scale. The relationship between the radius, r_p, of a pore opening and the pressure, P, needed to fill it is

$$P = -\frac{2\gamma}{r_p}\cos\theta \quad (1)$$

where γ is the surface tension of mercury (474 mN/m or dyne/cm at 25°C) and θ its contact angle on the surface of the adsorbent studied. In the absence of a better estimate, this angle is assumed to be 130°. Thus, under a pressure of 1 MPa (i.e., 10 kg/cm^2 or 142 p.s.i.), pores of 0.61 μm are filled. Eq. (1) is known as the Washburn equation.

Note that the contact angle is a function of temperature and pressure. During the measurement, the pressure is raised to approximately 410 MPa (ca. 60 000 p.s.i. or 4100 kg/cm^2). Because mercury is compressible, the temperature of the sample increases, by approximately 30°C. As a consequence, the contact angle varies systematically during the measurements. This introduces a systematic error

which cannot be corrected at present. This error is well reproducible for equipments of a given model. The variation of temperature is nearly independent of the sample because the heat capacity of mercury far exceeds that of the sample. The temperature dependence of the contact angle depends on the sample but is probably close for the four materials studied here. The pore size distributions are comparable. Except for the large mode of the pore size distributions, they are not accurate.

2.3. Nitrogen sorptometry

The amounts of nitrogen adsorbed are measured as a function of the partial pressure of nitrogen in a stream percolating through the sample. The surface area of the sample is derived using the BET method [13]. The adsorption and desorption isotherms of nitrogen determined following the same procedure are different. From these isotherms, information can be derived regarding the pore size distribution, using a suitable model. The model developed by Barrett et al. [14] is the most popular one at present and was used in this work (BJH method). It assumes that the pores are cylindrical and that the amount of adsorbate in equilibrium with the gas phase is retained in the pores of the adsorbent by two mechanisms, either physical adsorption on the pore walls or capillary condensation in the inner capillary volume. The BJH method can be applied to either the adsorption or the desorption isotherm. The desorption isotherm is preferred for comparison with the similar data obtained with mercury intrusion porosimetry because this isotherm corresponds to a lower energy, hence a more stable state [5].

2.4. Inverse size-exclusion chromatography

Solutions of polymeric samples of known average molecular mass and of low polydispersity are injected into the column studied. The mobile phase is chosen so as to minimize the possible interactions between the adsorbent surface and the samples. Retention has to be negligible. In the case of polystyrene samples dissolved in a nonpolar mobile phase (methylene chloride) and a C_{18} chemically bonded silica surface, the following correlation derived by van Kreveld and van den Hoed [6] and used by Halasz and Martin [7] relates the average molecular mass, M_{rn}, and the average diameter of the excluded pores, ϕ_n (the molecules with a molecular mass larger than M_{rn} are excluded from all pores smaller than ϕ_n).

$$\phi_n \simeq 0.621(M_{rn})^{0.588} \quad (2)$$

This equation allows the derivation of an approximate estimate of the pore size distribution from the determination of the retention volumes of a series of authentic samples [11]. It gives results which are different from those of nitrogen sorptometry [12]. Eq. (2) is approximate, even in the assumption that the polymer molecules are hard spheres [8], which they are certainly not. From early work by Cassasa [15] to the work by Knox and Scott [8] and the recent work by Vilenchik et al. [16], many authors have attempted, with limited success, to relate the pore size distribution of the pores of the packing material and the molecular characteristics of the polymer probes. For the purpose of this study, in which four similar materials are compared, it seems more appropriate to use an empirical approach than to attempt to correct the data when no satisfactory procedure is yet available to do so.

2.5. Definitions

Scheme 1 shows that we need to consider separately the inaccessible volume, V_s, the internal pore volume (inside the particles), $V_{p,i}$, and the

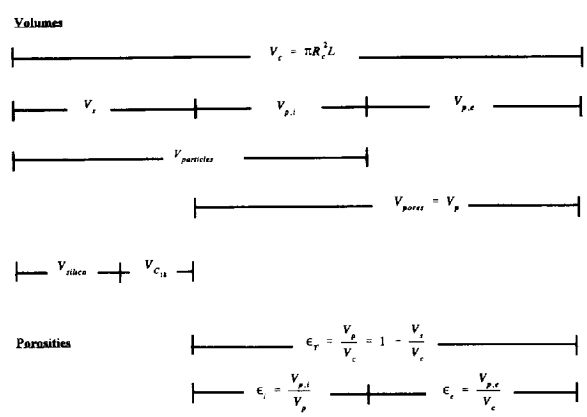

Scheme 1. Definition of the volumes and porosities used in this work.

external pore volume (around the particles), $V_{p,e}$. Two parameters are directly accessible to experimental determinations:

The inaccessible volume fraction, ϵ_U, and the inaccessible solid volume, V_s, which include the silica skeleton, the bonded alkyl layer and the non-connected or closed pores. The parameters characterizing this fraction of the column volume have been discussed previously [17] and are not within the scope of the present study. This fraction is directly measured by helium pycnometry.

The total porosity of the column or fraction accessible to the liquid phase, ϵ_T, and the total pore volume, V_p. The total porosity is derived from determinations of the column hold-up volume. It has been shown that there is a good agreement between the values of this hold-up volume derived from the retention volume of uracil in methanol–water mixtures and that of benzene in methylene chloride [17]. There is also an excellent agreement between the two parameters ϵ_U and ϵ_T, their sum being very close to unity.

The latter parameter, ϵ_T, is the sum of the column external and internal porosities. There is some ambiguity in the definitions of these last two parameters because it is impossible to define a sharp boundary between them. Previous work [11,17] has shown that a plot of the retention volume of polymeric fractions of known average molecular mass and low polydispersity versus the logarithm of their average molecular mass can be well accounted for by two straight lines, one of them being very steep, the second much less. From the coordinates of the intersect of these lines, it is possible to derive a plausible boundary between the size of the largest internal pores and that of the lowest external pores. This method was used here. The internal pore volume can also be derived from the data supplied by nitrogen sorptometry and mercury intrusion. Because all the measurements involved can be made quite accurately, the results of these three methods should agree. Our data support this conclusion (see Results and Discussion, Section 4.5).

2.6. Relationships

Experimental results obtained with series of five different columns packed with each one of the packing materials studied were presented previously [11]. Some of these results are reported in Tables 1–4 and compared with the values of the same parameters derived from the measurements reported in this work. We summarize here the relationships used in these determinations (see Scheme 1). The geometrical column volume is the sum of three main contributions:

$$V_c = V_s + V_i + V_e \tag{3}$$

including the unaccessible volume or volume occupied by the solid (silica, bonded material and possibly closed pores), the internal pore volume (inside the porous particles) and the external pore volume (around the particles). These contributions can be grouped by two, to obtain the particle volume ($V_p = V_s + V_i$) and the total volume occupied by the liquid ($V_T = V_i + V_e$).

The total column pore volume, V_T, is

$$V_T = V_c - V_s = V_c - \frac{W}{\rho_a} = \epsilon_T V_c \tag{4}$$

where W is the mass of stationary phase, determined by weighing the dried column and subtracting the mass of the empty tubing, ρ_a is the density of the packing material as obtained by helium pycnometry and ϵ_T, is the total porosity or fractional column volume available to the liquid phase.

The total volume of the internal pores of the material contained in the column, V_i, is obtained as the product of the mass of packing material in the column and the specific porosity, v_{BJH} (ml/g), derived from the data obtained by nitrogen sorptometry, using the BJH method

$$V_{p,i} = W v_{BJH} \tag{5}$$

The total volume of the internal pores is also obtained from ISEC data, as explained in the section above, and from mercury intrusion porosimetry (Section 2.2).

Finally, the total external pore volume in the column, V_e, is the difference between the column volume, V_c, and the total particle volume or sum of the solid volume ($V_s = W/\rho_a$) and the internal pore volume. Hence, the external porosity, ϵ_e, is given by

Table 1
Properties of the Kromasil columns

	Column					Average	R.S.D.[d] (%)
	1	2	3	4	5		
W (g)	1.1070	1.1287	1.1331	1.1374	1.1302	1.1273	0.95
V_s [a] (ml)	0.706	0.720	0.723	0.726	0.721	0.719	0.95
V_p (ml)	0.956	0.942	0.939	0.936	0.941	0.943	0.95
$V_{p,i}$ [b] (ml)	0.404	0.412	0.413	0.415	0.412	0.411	0.95
$V_{p,e}$ (ml)	0.552	0.530	0.526	0.522	0.529	0.532	2.0
Data, this work[c]							
ϵ_T [a]	0.575	0.566	0.565	0.563	0.566	0.567	0.7
ϵ_e	0.332	0.319	0.316	0.314	0.318	0.320	2.0
ϵ_i [b]	0.364	0.364	0.364	0.364	0.364	0.364	0.00
Previous data [10]							
ϵ_T (benzene)	0.608	0.597	0.598	0.595	0.595	0.5986	0.8
ϵ_i	0.365	0.36	0.361	0.361	0.359	0.3612	0.6
ϵ_e	0.383	0.37	0.371	0.366	0.368	0.3716	1.6
ϵ_T (uracil)	0.588	0.58	0.584	0.581	0.582	0.5830	0.3
Ratio previous data/data in this work							
ϵ_T (benzene)	1.057	1.053	1.058	1.056	1.051	1.055	0.3
ϵ_i	1.004	0.990	0.993	0.993	0.987	0.993	0.6
ϵ_e	1.153	1.159	1.172	1.166	1.156	1.161	0.6
ϵ_T (uracil)	1.016	1.023	1.035	1.031	1.026	1.026	0.7

Apparent density of the material by helium pycnometry, 1.5674 g/ml [13]; column volume 1.662 ml; porevolume from the BJH desorption isotherm, 0.3646 ml/g.

[a] From helium pycnometry data.

[b] From nitrogen sorptometry data.

[c] The sum of the internal and external porosity is not equal to the total porosity. See Eq. (6).

[d] R.S.D., relative standard deviation.

$$\epsilon_e = \frac{V_c - V_p}{V_c} = 1 - \frac{V_i + V_s}{V_c} = 1 - \frac{\frac{W}{\rho_a} + WV_{BJH}}{V_c}$$

$$= 1 - \frac{W}{V_c}\left(\frac{1}{\rho_a} + v_{BJH}\right) \quad (6)$$

The external porosity is obtained similarly from ISEC data and from the data on mercury intrusion.

The internal porosity, ϵ_i, of the column is given by

$$\epsilon_i = \frac{V_i}{V_p} = \frac{WV_{BJH}}{V_c(1 - \epsilon_e)} = \frac{v_{BJH}}{1/\rho_a + v_{BJH}} \quad (7)$$

The second equation results from the definition of the internal porosity as the ratio of the internal pore volume to the total volume of the particles [11].

Thus, the data obtained by helium pycnometry and nitrogen sorptometry allow the independent derivation of the internal and external porosity of each column. ISEC and mercury intrusion porosimetry supply similar data. The degree of agreement between these data of different origin is the main topic of this work. These data, their average value and standard deviation are reported in the Tables. They are also compared to the data obtained by conventional chromatographic methods.

3. Experimental

3.1. Samples

Samples of four different C_{18} ODS packing materials were obtained, Kromasil from Eka-Nobel (Stratford, CT, USA), Vydac from The Separation

Table 2
Properties of the Vydac columns

	Column					Average	R.S.D. (%)
	1	2	3	4	5		
W (g)	1.1269	1.1337	1.1132	1.1381	1.1277	1.1279	0.75
V_s [a] (ml)	1.047	1.050	1.043	1.052	1.048	1.048	0.75
V_p (ml)	0.615	0.612	0.619	0.610	0.614	0.614	0.75
$V_{p,i}$ [b] (ml)	0.458	0.461	0.453	0.463	0.459	0.459	0.75
$V_{p,e}$ (ml)	0.563	0.556	0.576	0.552	0.562	0.562	1.5
Data, this work[c]							
ϵ_T [a]	0.615	0.612	0.619	0.611	0.614	0.614	0.5
ϵ_e	0.339	0.335	0.347	0.332	0.338	0.338	1.5
ϵ_i [b]	0.417	0.417	0.417	0.417	0.417	0.417	0
Previous data [10]							
ϵ_T (benzene)	0.637	0.633	0.635	0.634	0.635	0.6348	0.2
ϵ_i	0.422	0.419	0.421	0.423	0.423	0.4216	0.35
ϵ_e	0.372	0.368	0.369	0.366	0.366	0.3682	0.6
ϵ_T (uracil)	0.634	0.632	0.638	0.634	0.641	0.6358	0.3
Ratio previous data/data in this work							
ϵ_T (benzene)	1.037	1.034	1.026	1.038	1.034	1.034	0.4
ϵ_i	1.012	1.005	1.010	1.014	1.014	1.011	0.35
ϵ_e	1.098	1.100	1.064	1.102	1.082	1.089	1.3
ϵ_T (uracil)	1.032	1.032	1.030	1.038	1.032	1.033	0.3

Apparent density of the material by helium pycnometry, 1.7589 g/ml [13]; column volume 1.662 ml; pore volume from the BJH desorption isotherm, 0.4068 ml/g.

[a] From helium pycnometry data.

[b] From nitrogen sorptometry data.

[c] The sum of the internal and external porosity is not equal to the total porosity. See Eq. (6).

Group (Hesperia, CA, USA), YMC from YMC (Wilmington, NC, USA) and Zorbax from BTR (Wilmington, DE, USA). All these materials have spherical particles, with a nominal 10 μm average particle size. For each material, samples of the same lot were used.

3.2. Chromatographic experiments

All these experiments were done with the same equipment and under the same conditions as described previously [11,17]. Five columns were packed and studied with each of the four packing materials. The data pertaining to each of those columns have been published and discussed in a previous publication [11]. Some of these data have been reproduced in Tables 1–4, when relevant to the present discussion and to the comparison of the results obtained by ISEC and by the other two techniques used here.

The column dimensions were measured and found to be the same for the 20 columns used: length 10 cm, inner diameter 4.6 mm, hence inner volume, $V_c = 1.662$ ml. This volume is in agreement with the difference between the masses of an empty column and of the same column filled with water, taking the density of water at room temperature into account. The tube constriction due to the tightening of the ferrules is estimated (from the diameter of the initial tubing and from the diameters of the final tubing at the mouth and at the ferrule level and from the ferrule length) to be of the order of 0.1%. This correction was neglected.

3.3. Measurement of the apparent density

The apparent densities of the packing materials

Table 3
Properties of the YMC columns

	Column					Average	R.S.D. (%)
	1	2	3	4	5		
W (g)	0.9037	0.8618	0.9557	0.8512	0.8641	0.8873	4.5
V_s [a] (ml)	0.564	0.538	0.597	0.531	0.540	0.554	4.5
V_p (ml)	1.098	1.124	1.065	1.131	1.122	1.108	2.7
$V_{p,i}$ [b] (ml)	0.554	0.528	0.586	0.522	0.530	0.544	4.5
$V_{p,e}$ (ml)	0.544	0.596	0.479	0.609	0.592	0.564	8.5
Data, this work[c]							
ϵ_T [a]	0.660	0.676	0.641	0.680	0.675	0.667	2.0
ϵ_e	0.327	0.358	0.288	0.366	0.357	0.339	8.5
ϵ_i [b]	0.495	0.495	0.495	0.495	0.495	0.495	0
Data, previous work [10]							
ϵ_T (benzene)	0.707	0.706	0.703	0.705	0.706	0.7054	0.2
ϵ_i	0.516	0.515	0.509	0.514	0.513	0.5134	0.5
ϵ_e	0.394	0.394	0.393	0.393	0.396	0.394	0.3
ϵ_T (uracil)	0.698	0.701	0.697	0.697	0.700	0.6986	0.2
Ratio previous data/data in this work							
ϵ_T (benzene)	1.070	1.044	1.097	1.036	1.045	1.059	2.0
ϵ_i	1.042	1.040	1.027	1.038	1.036	1.036	0.5
ϵ_e	1.200	1.100	1.360	1.070	1.110	1.170	9.0
ϵ_T (uracil)	1.057	1.037	1.087	1.025	1.036	1.048	2.0

Apparent density of the material by helium pycnometry, 1.6016 g/ml [13]; column volume 1.662 ml; pore volume from the BJH desorption isotherm, 0.6130 ml/g.

[a] From helium pycnometry data.

[b] From nitrogen sorptometry data.

[c] The sum of the internal and external porosity is not equal to the total porosity. See Eq. (6).

were determined by pycnometry, using an ACCUPYC 1330 (Micromeritics, Norcross, GA, USA). The experiments were carried out as previously described [3,11,17]. These data are reported in Tables 1–4. The data were further interpreted using the percentage of carbon bonded to the silica, as supplied by the manufacturer. The density of the bonded layer was assumed to be the same as that of liquid octadecane. Because all the alkyl chains are bonded to the surface, the density is probably lower, as suggested by the important increase of the partial molar volume of a CH_2 group associated with its passage from a water–methanol solution to the bonded layer [18].

3.4. Mercury intrusion porosimetry

The determinations of the pore size distribution by mercury intrusion were carried out using an automated mercury porosimeter, AUTOPORE III 9420 (Micromeritics). This equipment is computer controlled and supplies directly the cumulative and incremental intrusion volumes as a function of the pore diameter, derived from the applied pressure using Eq. (1). The corresponding distribution of the surface area is derived assuming the pores to be cylindrical.

3.5. Nitrogen sorptometry

The nitrogen adsorption and desorption isotherms were determined using an ASAP 2400 (Micromeritics). This equipment supplies automatically the adsorption and desorption isotherms and calculates the BET surface area, the total volume of pores with less than 7344 Å diameter, the BJH cumulative adsorption and desorption surface areas and the BJH cumulative adsorption and desorption pore volumes

Table 4
Properties of the Zorbax columns

	Column					Average	R.S.D. (%)
	1	2	3	4	5		
W (g)	1.2513	1.2583	1.2651	1.2804	1.2539	1.2618	0.8
V_s [a] (ml)	0.694	0.698	0.701	0.710	0.695	0.699	0.8
V_p (ml)	0.968	0.964	0.961	0.961	0.967	0.963	0.8
$V_{p,i}$ [b] (ml)	0.367	0.369	0.371	0.375	0.368	0.370	0.8
$V_{p,e}$ (ml)	0.602	0.596	0.590	0.577	0.599	0.593	1.5
Data, this work[c]							
ϵ_T [a]	0.583	0.580	0.578	0.573	0.582	0.579	0.6
ϵ_e	0.362	0.358	0.355	0.347	0.361	0.357	1.5
ϵ_i [b]	0.346	0.346	0.346	0.346	0.346	0.346	0
Previous data [10]							
ϵ (benzene)	0.603	0.606	0.599	0.603	0.600	0.6022	0.4
ϵ_i	0.338	0.342	0.337	0.340	0.335	0.3384	0.7
ϵ_e	0.399	0.401	0.395	0.398	0.398	0.3982	0.5
ϵ_T (uracil)	0.593	0.595	0.590	0.594	0.590	0.5924	0.35
Ratio previous data/data in this work							
ϵ_T (benzene)	1.035	1.044	1.036	1.053	1.031	1.040	0.75
ϵ_i	0.977	0.989	0.974	0.983	0.969	0.978	0.7
ϵ_e	1.102	1.119	1.113	1.147	1.104	1.117	1.5
ϵ_T (uracil)	1.018	1.025	1.021	1.037	1.014	1.023	0.8

Apparent density of the material by helium pycnometry, 1.8039 g/ml [13]; column volume 1.662 ml; pore volume from the BJH desorption isotherm, 0.2931 ml/g.

[a] From helium pycnometry data.

[b] From nitrogen sorptometry data.

[c] The sum of the internal and external porosity is not equal to the total porosity. See Eq. (6).

for pores between 17 and 3000 Å in diameter. The incremental surface areas ($dA/d\log(D)$ and dA/dD) and incremental pore volumes ($dV/d\log(D)$ and dV/dD) are also supplied. The global data obtained are summarized in Tables 1–4. The distributions are reported and compared in the Figures. Both adsorption and desorption isotherms were used to calculate the pore size distribution using the BJH method.

3.6. Description of the tables

For each packing material studied, five columns have been packed. The first row in the corresponding table gives the mass of packing material contained in the column, determined as the difference between the mass of the empty tubing and the mass of the column dried after completion of all measurements [11]. The second row gives the volume of solid packing in the column, V_s, derived from the packing mass and its apparent density obtained by helium pycnometry [17]. The third row gives the total pore volume, V_p, as the difference between the geometrical column volume ($\pi d_c^2 L/4 = 1.662$ ml) and the volume of solid packing. The fourth row gives the internal pore volume, V_i, derived from the nitrogen porosimetry data. The fifth row gives the external pore volume, V_e, as the difference between the total pore volume (third row) and the internal pore volume (fourth row). In a second block of numbers, the total (ϵ_T), external (ϵ_e) and internal (ϵ_e) porosities are given, as derived from the volumes reported in the first block of numbers and the geometrical volume of the column. The third block of data contains the values of the same total, internal and external porosities determined on the same columns, using only chromatographic methods (i.e., using the ISEC data), hence using an independent approach. Finally, the

fourth block of data gives the ratio of the values of the porosities determined in this work and in the previous report [11].

4. Results and discussion

The results obtained are summarized in Tables 1–4 (corresponding to the different packing materials studied), in Figs. 1–3 (corresponding to the different techniques used) and in Figs. 4–7 (corresponding to the different packing materials studied). We first discuss separately the results obtained with each method and then compare them for the different materials. The different principles of the methods used introduce different limitations, uncertainties and thresholds.

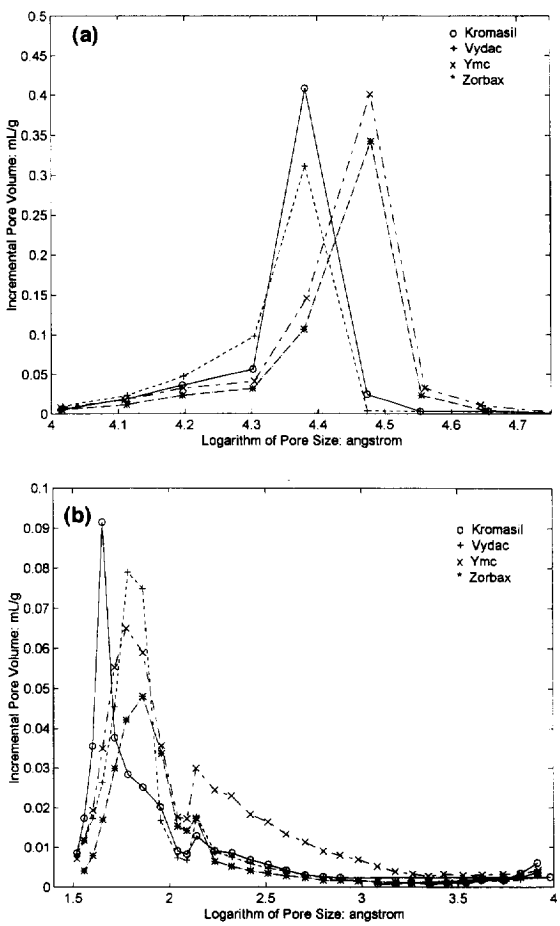

Fig. 1. Pore size distribution obtained by mercury intrusion porosimetry for the four packing materials studied. (a) High pore size mode, above 1000 Å. (b) Low pore size mode, below 1000 Å.

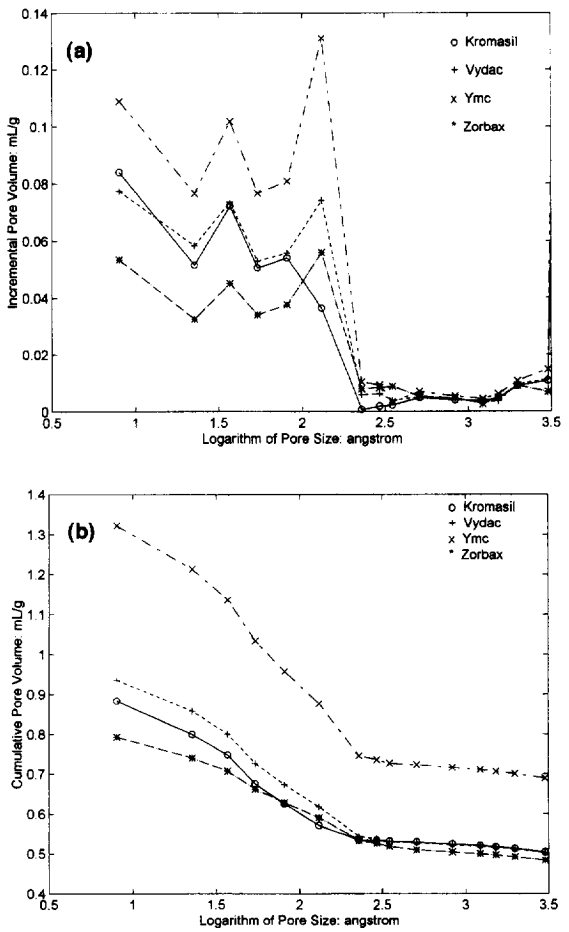

Fig. 2. Pore size distribution derived from the chromatographic data obtained by ISEC, for the four packing materials studied. Note the small number of data points obtained for the high pore size mode. (a) Incremental distribution. (b) Cumulative distribution.

4.1. Mercury intrusion porosimetry

The distributions obtained (Fig. 1a,b) are bimodal. Obviously, the large-size mode corresponds to the external pores between particles, the low-size mode to the internal pores, within the packing particles.

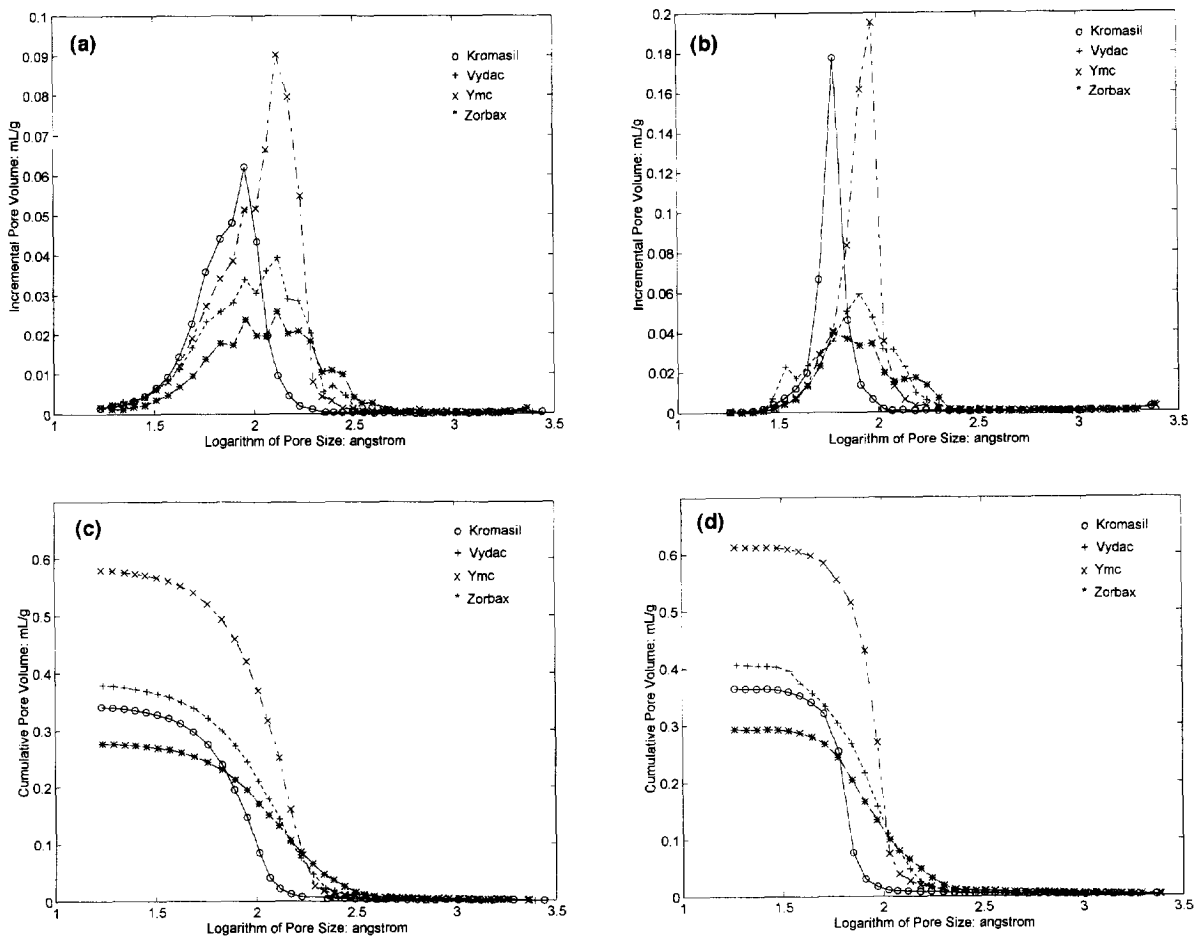

Fig. 3. Size distribution of the internal pores of the four packing materials studied obtained by nitrogen sorptometry. (a) Incremental distribution derived from the nitrogen adsorption isotherm. (b) Incremental distribution derived from the nitrogen desorption isotherm. (c) Cumulative distribution derived from the nitrogen adsorption isotherm. (d) Cumulative distribution derived from the nitrogen desorption isotherm.

Although contributions to the pore volume could be measured for pores as large as 120 μm in diameter, only a negligible contribution was observed above 4.5 μm, which seems to be quite reasonable for 10 μm particles. For all samples, the incremental contribution is very low between 0.1 and 1 μm, with a minimum between 0.2 and 0.3 μm which is slightly higher for YMC than for the other three materials. Both the high and the low modes of the distribution are different for the four samples, For the sake of clarity, these modes are presented separately in Fig. 1a (high pore size mode) and Fig. 1b (low pore size mode)[1]. This enhances the differences between the results obtained with the four different packing materials.

We note that the profiles of the high-size mode for the four different samples studied (Fig. 1a) are much

[1] The reader should remember that (1) the pore size distributions shown in this work are histograms; (2) the abscissa scale is semi-logarithmic; and (3) the density of data points is linear. Accordingly, there is little relationship between the true porosity (an integral of pore density versus pore volume) and the apparent area of the curves (an integral of pore density versus the logarithm of the pore size).

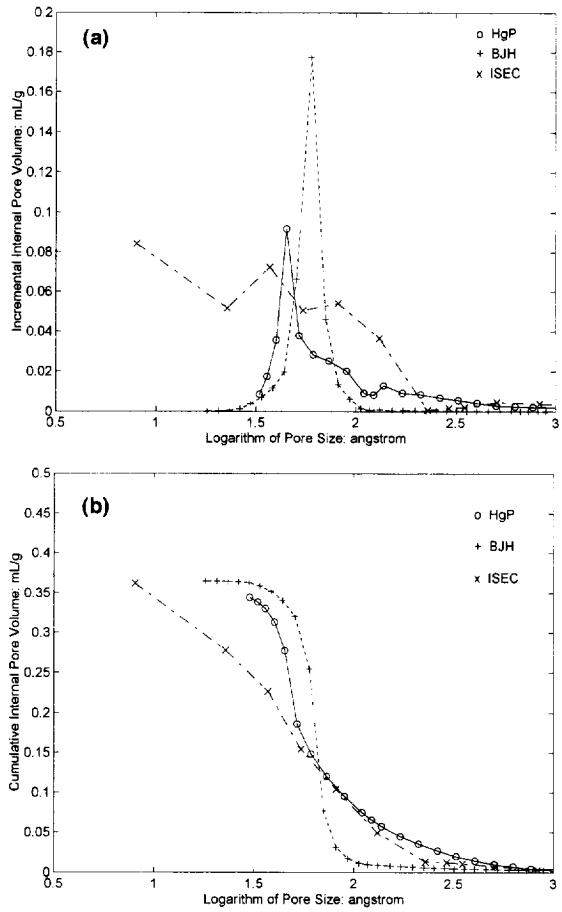

Fig. 4. Comparison of the size distributions of the internal pores obtained by the three different methods for Kromasil. (a) Incremental distribution for the low pore size mode. (b) Cumulative distribution for the low pore size mode.

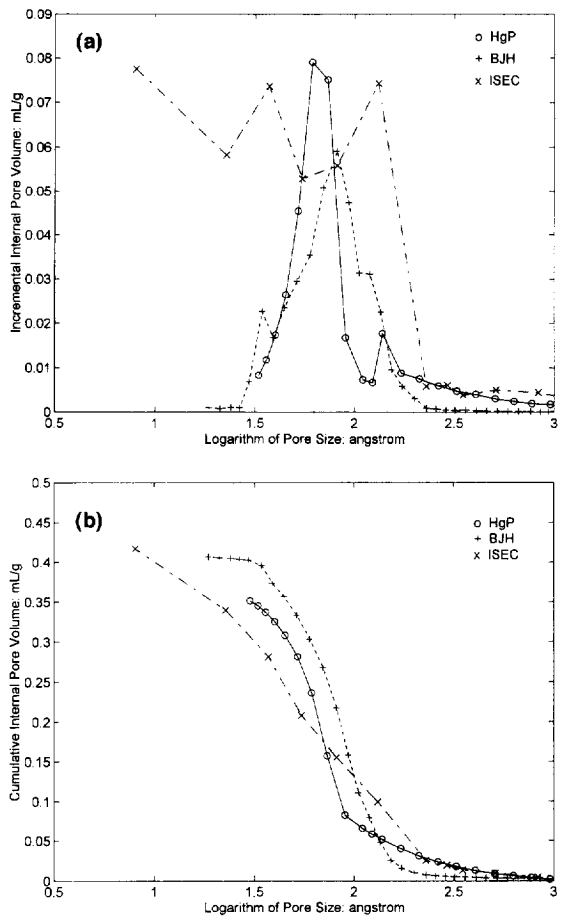

Fig. 5. Comparison of the size distributions of the internal pores obtained by the three different methods for Vydac. (a) Incremental distribution for the low pore size mode. (b) Cumulative distribution for the low pore size mode.

less different than the profiles obtained for the low-size mode (Fig. 1b). For the high-size mode, the shift between the position of the mode maximum for Kromasil and Vydac (at 2.04 μm) and for YMC and Zorbax (at 3.01 μm) is one single data interval, hence marginally significant. It could be explained by a slightly larger average particle diameter for the particles of the last two materials compared to those of the first two ones or by the presence of a small fraction of particle agglomerates. This result is expected since the four samples are made of nearly spherical particles with a relatively narrow particle size distribution [17]. The front of the distribution on the high-size side is very steep, nearly vertical for all four materials. The external pore size distribution is significantly narrower for Kromasil and Vydac than for the other two materials and its tail is less important for Kromasil, which is made of nearly spherical particles, than for Vydac [17]. The characteristics of the mode profiles, like the differences between the compression dynamics of the packing materials [19], are related to the smoothness of the particles and the deviation of their shape from that of a sphere. The model developed by Mayer and Stowe [20] and relating mercury intrusion data and particle size distribution could be used for a refined analysis

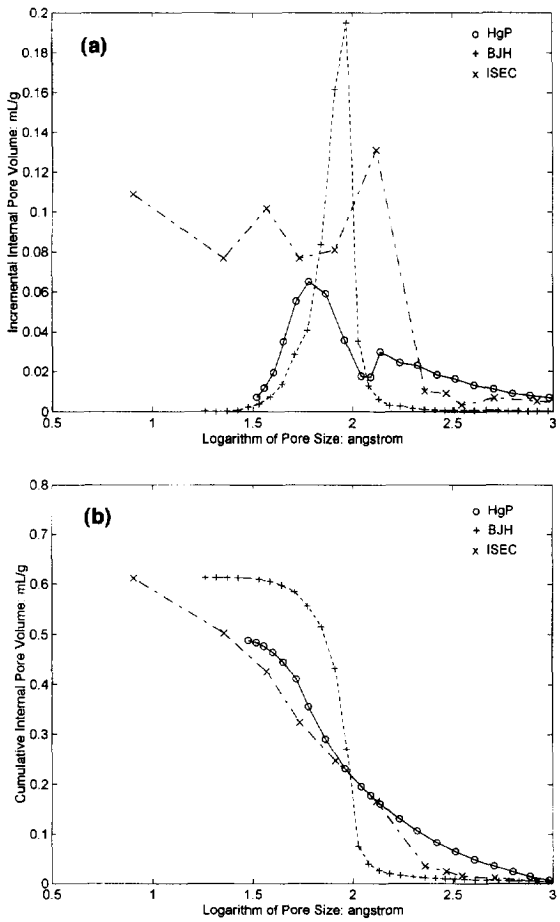

Fig. 6. Comparison of the size distributions of the internal pores obtained by the three different methods for YMC. (a) Incremental distribution for the low pore size mode. (b) Cumulative distribution for the low pore size mode.

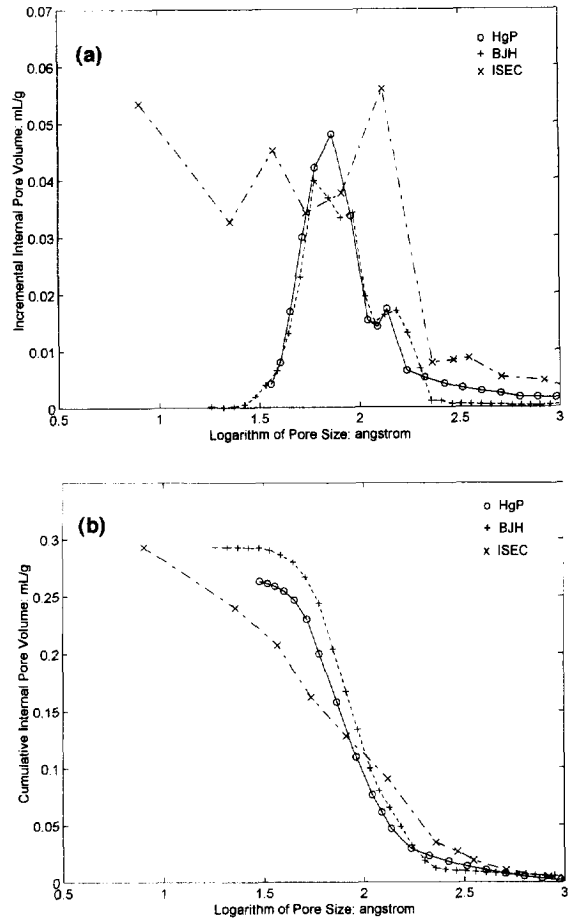

Fig. 7. Comparison of the size distributions of the internal pores obtained by the three different methods for Zorbax. (a) Incremental distribution for the low pore size mode. (b) Cumulative distribution for the low pore size mode.

of the experimental results reported. This did not seem to be warranted at this stage.

By contrast, the profiles of the low-size mode of the pore size distributions (i.e., the pore size distribution of the internal porosity) are quite different, reflecting the differences in the internal structures of these different particles (Fig. 1b). Zorbax has a narrower, sharper distribution, with practically no pores beyond 200 Å (in this internal porosity mode). Kromasil has a sharp maximum at a lower pore size (45 Å) than the other three materials (for which the maxima are located between 60 and 70 Å). All materials, even Zorbax, have a small satellite mode around 140 Å. This mode is more important for the YMC material, but exists in all of four packing materials.

4.2. Inverse size-exclusion chromatography

Pore size distributions similar to those obtained by mercury intrusion porosimetry had been reported previously as the results of determinations carried out with ISEC [11,17]. The distributions obtained with ISEC are reported in Fig. 2a (incremental distribution) and Fig. 2b (cumulative distribution of the total porosity). They exhibit also two well separated modes, although a comment is necessary. ISEC exhibits no resolution for pore sizes above ca.

1500 Å, as illustrated by the plateau in the high pore size range in Fig. 2b. This plateau ends at the largest pore size measurable by ISEC, short of the beginning of the high pore-size mode. The minimum between these two modes is located around 0.15 μm, except for Kromasil where it is lower, around 250 Å [11]. Even in the latter case, however, the contribution of the external porosity mode is negligible below 0.5 μm. Note also that all the distributions are flat and low between approximately 200 and 1500 Å. As seen later, nitrogen sorptometry does not allow the determination of any accurate estimate of the high pore-size mode of the pore size distribution either. Only the mercury intrusion porosimetry data are useful in this range.

As previously reported by Knox and Scott [8], the pore size distribution derived from Mercury intrusion porosimetry (Fig. 1a,b) has always a steeper dependence on the pore size than the distribution derived from the chromatographic data (Fig. 2). This is particularly noticeable for the low-size mode, possibly because the number of data points obtained in ISEC for the high-size mode is too small to accurately represent the pore size distribution. Note also that the density of data points in the ISEC distribution is much lower than for the mercury intrusion porosimetry measurements. Although the data are represented as broken straight lines in the Figures, they are really histograms. The actual porosities resulting from mercury intrusion porosimetry and ISEC are quite close (see Tables 1–4, Fig. 2b) although the area under the less dense ISEC distribution (Fig. 2a) appears much higher at first glance.

The cumulative pore size distributions obtained for Kromasil, Vydac, YMC and Zorbax are very close (Fig. 2b). The distribution for the YMC material is well above the other three, reflecting the higher internal porosity of this adsorbent. However, the shift observed in the large pore size range (above ca. 300 Å) is in part due to the choice of reporting the porosity data as pore volume per unit mass of the packing material. Since YMC has a larger internal porosity than the other three adsorbents [11], its apparent density is lower and a much larger number of particles is needed to make 1 g of packing material. This is illustrated by a mass of packing in the YMC packed columns which is quite lower than in the columns packed with the three other materials. Hence the larger external pore volume of the YMC columns.

4.3. Nitrogen sorptometry

The contribution of the outside surface area of the particles to their total specific surface area is so small that it is negligible compared to the experimental error[2]. So is the contribution of this external surface area to adsorption. Accordingly, it is not possible to obtain with a sorptometric method any estimate of the external or high-size mode of the pore size distribution.

The incremental or differential distributions of the low pore size contributions as a function of the pore size are reported in Fig. 3a,b for the four samples (see footnote in Section 4.1). The data in these two figures were obtained by applying the BJH method to the adsorption and the desorption isotherm, respectively. The cumulative or integral pore volume distributions by pore size are reported in Fig. 3c,d, respectively. The volume based distributions are wider for Vydac and Zorbax than for Kromasil and YMC. Kromasil has a lower average value of the pore size than the other three materials which seem to have similar size. The YMC material has a higher internal porosity than the other three materials, because of the long tail of the satellite mode toward the high pore size. There are significant differences between the pore size distributions derived from the adsorption (Fig. 3a,c) and the desorption (Fig. 3b,d) isotherms. The adsorption isotherm gives wider, shorter distributions than the desorption isotherm. The maxima of the distributions derived from the desorption isotherms correspond to slightly smaller pore sizes than those derived from the adsorption isotherms.

Because the pore size distributions derived from the desorption isotherms are much closer to the distributions derived from mercury intrusion data, these distributions, rather than those derived from the adsorption isotherms, will be used in the comparisons of the pore size distributions afforded by

[2] The total surface area corresponding to pores larger than the threshold of 1500 Å adopted as the boundary between internal and external pores is given in Tables 1–4 for illustration.

different methods for the phases studied (see Sections 4.7–4.11). This choice is supported by the literature [5]. The pore surface area distributions derived from the desorption isotherms are discussed later in this report.

4.4. External pore size distribution

In order to allow comparison of the data obtained with the three methods, we decided arbitrarily to assign all the contributions below 1500 Å to the inner porosity and those above to the external porosity (this does not apply to nitrogen sorptometry, the method giving no data for external porosity). In view of the excellent resolution between the two modes of the pore size distribution observed (see Section 4.3), this choice of 1500 Å has little consequences on the overall results. The profiles of the high-size mode of the pore size distributions obtained by mercury intrusion porosimetry and by ISEC cannot be compared directly because of the lack of discrimination of the ISEC data. The former method gives 12 to 15 data points in the pore size range of 0.35 to 6.0 μm in which this mode is located, the latter method only two. ISEC is more suitable for the determination of the internal porosity than for that of the profile of the high pore-size mode of the pore size distribution, although it is not the best method, as seen later. The data in the Tables show that there is an excellent agreement between the values of the internal porosity determined by chromatographic methods (hold-up volume and ISEC data, respectively) and by nitrogen sorptometry or mercury intrusion porosimetry (see Sections 4.7–4.10). There is also a good agreement between the values of the total porosity obtained by these two methods. In almost all cases, however, the chromatographic data regarding the total and the external porosities are systematically high. This could have been explained by an insufficient correction for the extra-column volume of the equipment or dead volume. However, this explanation must be ruled out because a value of the dead volume correction was determined at the beginning of each new series of measurements, between the time when a column was taken away from the instrument and the time when the new column was fastened.

There is an important difference between the values of the external porosity derived from the parameters the measurements of which are reported here and those determined by chromatographic methods. This difference must be contrasted with the excellent agreement between the values of the internal porosities obtained using the same sets of data. The chromatographic values of the external porosities are 9 to 17% higher than the values calculated from the solid volume (measured by helium pycnometry) and the internal pore volume (determined by nitrogen sorptometry). Note that part of the difference is explained by a larger total porosity derived from the retention time of benzene in a nonpolar solvent than the one derived from the retention time of uracil in a methanol–water solution. One would have rather expected a difference in the internal porosity, related with a different structure of the bonded layer of alkyl chains in these two solvents.

Errors on the column length or on the correction for the extra-column dead volume are ruled out by the reproducibility of the external porosity obtained by chromatographic methods (approximately 1%). The external porosity is derived (Eq. (5)) from the value of four parameters, the mass of packing material in the column, the column inner geometrical volume, the apparent density of the packing material (in a gas phase) and the specific internal pore volume. It has been shown elsewhere [21] that the packing mass obtained by the procedure used here is the same as the mass of the oven-dry packing obtained using the conventional method, within a fraction of 1% including losses during column unpacking needed in the conventional method. Helium pycnometry is a straightforward, absolute method, with no model error and requiring simple calibration. The results are reproducible within 0.1%. The agreement between the values of the internal porosity derived from ISEC and nitrogen sorptometry suggests that there is only a small error on the value of V_{BJH}. The exactness of the value used for the column volume was checked by measuring the masses of an empty column and of the same column filled with water. The result agrees with the geometrical volume calculated.

This leaves us with the suggestion that benzene in a dichloromethane solution, and uracil in methanol are not completely unretained as claimed in the

literature but have a small retention factor. In this case, the retention factor would be the difference between the ratio of the values of ϵ_T derived from the retention volume of benzene or uracil, respectively, and measured in this work (Tables 1–4, lines 1 and 4 from bottom) minus 1. The retention factors of benzene and uracil would thus be approximately 0.05 and 0.03 on Kromasil, respectively, 0.03 and 0.03 on Vydac, 0.06 and 0.05 on YMC, 0.04 and 0.025 on Zorbax. The precision of this determination is low, no better than ca 10%. This assumption seems reasonable and is no way in contradiction with the literature, the experimental difficulties in the measurement of such small retention factors being obvious. The practical consequences of this result for most applications in which benzene or uracil are used as tracers of an unretained component under the same experimental conditions as used here would be negligible.

4.5. Internal pore size distribution

The profiles of the low-size mode of the pore size distributions obtained by mercury intrusion and by ISEC and of the volume pore size distribution derived from the data obtained by nitrogen sorptometry[3] (desorption isotherms) are reported in Figs. 4–7. Separate figures correspond to each of the four packing materials. The incremental and cumulative distributions are given successively. The internal pore volume has been defined as the volume of pores below 1500 Å, in agreement with the ISEC results [17]. mercury intrusion porosimetry supplies the pore volume down to 30 Å. ISEC allows determinations down to 8 Å, but with only 5 data points below 100 Å, for the lack of more suitable polystyrene samples. nitrogen sorptometry gives data down to 16 Å. This explains some discrepancies between the data obtained with the three methods at the low end of the distribution, a small, yet significant fraction of the pores of the samples studied being below 30 Å. There is a substantial, if not excellent, agreement between the distributions provided by the three different methods used. These differences are discussed later, on a case by case basis. We note that the distribution determined from the ISEC data is always the less steep of the three.

The pore sizes determined by mercury intrusion porosimetry tend to be slightly smaller than those derived from nitrogen sorption data. For example, the maximum of the mode for Kromasil is at 45 Å in the incremental distribution determined by mercury intrusion, at 90 Å in the distribution derived from the nitrogen adsorption isotherm (Fig. 3a) and at 60 Å in the distribution derived from the desorption isotherm (Fig. 3c, Fig. 4a). Similarly, the maximum of the incremental distribution determined by mercury intrusion porosimetry for the other three packing materials is at 60 to 70 Å while it is around 125 Å for the distributions derived from the nitrogen adsorption isotherms (Fig. 3a) and at 90 Å for the distributions derived from the nitrogen desorption isotherms (Fig. 5a to Fig. 7a).

The differences between the shape and the position of the maxima of the distributions derived from the adsorption and the desorption isotherms have been discussed earlier. The differences between the distributions derived from the nitrogen desorption isotherm and from the mercury intrusion data could be explained in part by the use of a slightly incorrect (i.e., too small) value of the contact angle of mercury on the surface of the C_{18} chemically bonded silica. Note, however, that this would be an empirical correction and that there are no fundamental reasons to do that. Furthermore, this systematic error alone cannot explain all the magnitude of the difference observed in the case of the distributions derived from the adsorption isotherms (a cosine has to be smaller than 1.0). Finally, (see Eq. (1)) the pore radius is proportional to cos θ, and this empirical recalibration could not change the shape of the distributions while these shapes are quite different, depending whether adsorption or desorption isotherms are used (cf. Fig. 3a,b). More probably, the explanation of the difference is in the finite elasticity of the particle walls between pores. These walls are strained by the high stress generated by the high external pressure of mercury around the necks of empty pores. Although we are in the realm of classical physics, this is a typical case in which the process of measuring a parameter actually changes it.

[3] As explained earlier, this method does not give any information regarding the distribution of the extra-particle pores because the contribution of these pores to the specific surface area is negligible.

The agreement between the values of the internal porosity derived for the same packing material by two independent methods, the measurements of the packing density by helium pycnometry and of the internal pore volume by nitrogen sorptometry on the one hand, ISEC on the other is impressive (Tables 1–4). The ratio between these two sets of values are 0.99, 1.01, 1.03 and 0.98 for Kromasil, Vydac, YMC and Zorbax, respectively, with small relative standard deviations of 0.6, 0.3, 0.5 and 0.7%, respectively. It would not be realistic to expect a better agreement, if only because of the limited accuracy of ISEC. The R.S.D. (relative standard deviation) on these data, which arises from the errors of measurement made in chromatography alone, accounts for a significant fraction of the difference between the two sets of results, except for the YMC material. Note also that if we accept the threshold of 1500 Å for the boundary between internal and external porosities, the data obtained by mercury intrusion are in very good agreement with the data obtained by the other two methods (Figs. 4b, 5b, 6b and 7b).

4.6. Cumulative distributions of the internal porosity

To further compare the four different materials studied, the cumulative distributions of the pore volume obtained with the three different methods are illustrated in Figs. 4b, 5b, Fig. 6b and 7b, corresponding to the internal pore size distributions. The cumulative distributions of the surface area are illustrated in Fig. 8a–d, corresponding to the four packing materials.

4.7. Pore size distributions of Kromasil

The profiles of the low-size mode of the incremental and cumulative pore size distributions (internal pore volume only) obtained for Kromasil with the three different methods used are compared in Fig. 4a and b, respectively. There is an excellent agreement between the values of the internal porosity derived by the different procedures used but a 16% difference between the estimates of the external porosity (Table 1). The values of the distribution of the pore sizes by volume derived by ISEC, although giving values of the porosity in agreement with those afforded by the other two methods, correspond to sizes which are too low, lower than the values determined by mercury intrusion (Fig. 4a). We note also that the steepness of the cumulative pore size distributions given by the three methods is quite different (Fig. 4b). The distribution derived from the results obtained by mercury intrusion porosimetry is as steep as the distribution afforded by nitrogen desorption (although it is quite steeper than the distribution derived from the nitrogen adsorption isotherm, Fig. 3c). ISEC gives the less steep of the three distributions. Note also that mercury intrusion porosimetry gives a bimodal distribution with the smaller mode at 140 Å, the most important mode at ca. 45 Å, a very steep profile toward the low pore sizes and a tail toward the high sizes (Fig. 4a). This tail is poorly separated from the second mode. By contrast, nitrogen adsorption gives a unimodal distribution, steep toward the high pore sizes where it ends around 100 Å and nearly as steep as the mercury intrusion distribution on the side of the low pore sizes. The distribution is much taller because it is narrower.

4.8. Pore size distributions of Vydac

The profiles of the low-size mode of the incremental and cumulative pore size distributions (internal pore volume only) obtained for Vydac with the three different methods used are compared in Fig. 5a and Fig. 5b, respectively. Most of the conclusions regarding the three distributions are similar to those derived in the previous case. The cumulative distribution obtained by mercury intrusion porosimetry is as steep as the distribution derived from the nitrogen desorption data and steeper than the distribution obtained from ISEC, which raises very slowly (Fig. 5b). The values of the total internal porosity obtained with the three methods are in excellent agreement, the slightly higher value obtained with ISEC (Table 2, Fig. 5b) could be explained by a low residual adsorption. Mercury intrusion porosimetry gives a bimodal pore size distribution with maxima at 65 and 135 Å (Fig. 5a). The main mode is rather narrow. Nitrogen sorptometry gives a broader, unimodal distribution with a maximum around 80 Å.

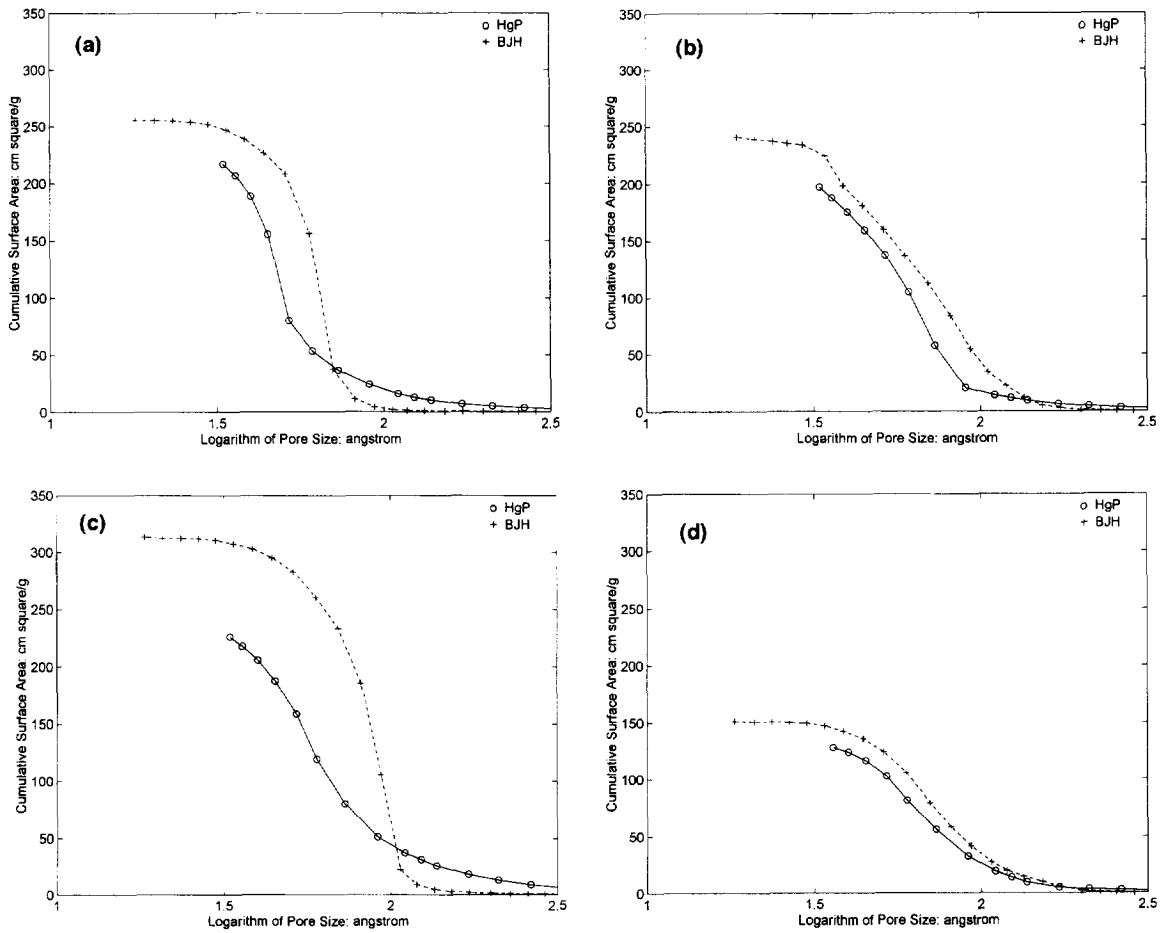

Fig. 8. Comparison of the surface area distributions by pore size obtained by mercury intrusion porosimetry and nitrogen sorptometry (desorption isotherm). (a) Cumulative distribution of Kromasil. (b) Cumulative distribution of Vydac. (c) Cumulative distribution of YMC. (d) Cumulative distribution of Zorbax.

4.9. Pore size distributions of YMC

The profiles of the low-size mode of the incremental and cumulative pore size distributions (internal pore volume only) obtained for Vydac with the three different methods used are compared in Fig. 6a and Fig. 6b, respectively. The characteristics of the columns packed with this materials are reported in Table 3. By contrast with the results obtained for the Kromasil and Vydac packing materials studied, the cumulative pore size distribution determined by nitrogen desorption is steeper than the one obtained by mercury intrusion porosimetry (Fig. 6b). It is also much narrower. The value of the internal porosity obtained with mercury intrusion porosimetry is lower than the values obtained with the other two techniques (Fig. 6b). Again, mercury intrusion porosimetry gives a bimodal distribution, with maxima at 50 and 130 Å, while nitrogen sorptometry gives a unimodal distribution with a maximum at 90 Å (Fig. 6a). This unique distribution mode is narrower than either of the two modes of the distribution obtained by mercury intrusion.

4.10. Pore size distributions of Zorbax

The profiles of the low-size mode of the incremen-

tal and cumulative pore size distributions (internal pore volume only) obtained for Zorbax with the three different methods used are compared in Fig. 7a and Fig. 7b, respectively. The characteristics of the packing are summarized in Table 4. Similar observations are made as for Kromasil and Vydac, the cumulative distributions derived from mercury intrusion data and from the nitrogen desorption isotherm are as steep, steeper than the ISEC distribution. The three values derived for the internal porosity are in good agreement, with the one obtained by mercury intrusion porosimetry slightly lower than the other two (Fig. 7b). The pore size distribution obtained by mercury intrusion porosimetry is again bimodal, with maxima at 75 and 135 Å. The distribution obtained by nitrogen is also bimodal, the two maxima, at 60–70 and 150 Å being very close to those of the other distribution (Fig. 7a). Zorbax has a lower internal porosity than the other three packing materials, hence its pore network could be less deformed under mercury compression.

4.11. Surface area distributions

Mercury intrusion porosimetry and nitrogen sorptometry allow the determination of the surface area of a material as a function of the pore size. Fig. 8a–d compare the area distributions obtained by the two techniques for each of the four packing materials. The contribution of the large external pores to these distributions is negligible, so the data shown corresponds essentially to the distribution of the internal pore surface area. Note that the values of the surface areas have been calculated assuming the conventionally accepted value of 16.2 $Å^2$ for the area occupied by one molecule of nitrogen when adsorbed on a solid surface. The accuracy of this value has been recently questioned by Jelinek and Kovats [22] who suggested 13.5 $Å^2$ instead.

Comparison between the data obtained with the two techniques on each packing material shows a very good agreement regarding the value of the internal porosity contrasting with a surprisingly large difference between the profiles of the cumulative distributions supplied by the two different techniques, mercury intrusion porosimetry giving distributions much steeper than nitrogen sorptometry. This suggests that a large fraction of the surface area is accessible only through relatively narrow openings.

5. Conclusion

The experimental results obtained with the three different methods of measurement of pore size distributions studied and the four different packing materials used are in excellent agreement. The differences observed, although quantitatively significant, would not cause any modification of the qualitative conclusions of a study aiming at comparing the characteristics of the four packing materials which would use only one of these methods for the determination of the pore size distribution. For the internal porosity, the differences between the results of the three methods are of the order of 1 to 2%, with an rstd between 0.3 and 0.7%.

It is clear, however, that ISEC cannot give any accurate data regarding the pore size distribution in the high-size range corresponding to the external porosity of the column and that, in the low-size range, it is only marginally useful. On the other hand, this method gives an accurate value of the external column porosity. Because of the ease and accuracy with which it allows this determination, this will probably be the most important practical application of ISEC, a result independently observed by Dunlap and Carr [12].

Finally, our data are compatible will very small but finite values for the retention factor of benzene in dichloromethane and uracil in methanol. These values are of the order of 0.04 to 0.05 for benzene and approximately 0.03 for uracil on the four packing materials, slightly higher on YMC than on the other three adsorbents. The reproducibility of the data acquired appears to be extremely good, with relative standard deviations on the various porosities which are almost always lower than 1%, probably in a large part because of the superb control of the flow-rate delivered by our chromatograph. This suggests a precision of the order of 10 to 20% on these estimates. Because these retention factors result from a material balance and that the different methods used to estimate the components of this balance are known to be sufficiently accurate, we consider the

values reported above as significantly different from 0.

Acknowledgments

We are grateful to Klaus Lohse (BTR, Wilmington, DE, USA), Per Jageland (Eka-Nobel, Stratford, CT, USA), Yan-Bo Yang (Vydac, Hesperia, CA, USA), and Robert Cooley (YMC, Wilmington, NC, USA) for their help and suggestions and for the gift of the ODS packing materials used throughout our studies. This work was supported in part by grant CHE-9201663 from the National Science Foundation and by the cooperative agreement between the University of Tennessee and the Oak Ridge National Laboratory.

References

[1] P.W. Carr, D.E. Martire and L.R. Snyder, J. Chromatogr. A, 656 (1994) 1.
[2] A.I. Liapis, Math. Modeling Sci. Computing, 1 (1993) 397.
[3] C. Orr Jr., Powder Technol., 3 (1969–70) 117.
[4] K.S.W. Sing, D.H. Everett, R.A.W. Haul, L. Moscou, R.A. Pierotti, J. Rouquerol and T. Siemieniewska, Pure Appl. Chem., 57 (1985) 603.
[5] S.J. Sing and K.S.W. Gregg, Adsorption Surface Area and Porosity, Academic Press, New York, 1982.
[6] M.E. Van Kreweld and N. Van den Hoed, J. Chromatogr., 83 (1973) 111.
[7] I. Halasz and K. Martin, Angew. Chem., Intl. Ed. Engl., 17 (1978) 901.
[8] J.H. Knox and H.P. Scott, J. Chromatogr., 316 (1984) 311.
[9] W.W. Yau, J.J. Kirkland and D.D. Bly, Modern Size-Exclusion Chromatography, Wiley, New York, 1979.
[10] M. Czok and G. Guiochon, J. Chromatogr., 506 (1990) 303.
[11] H. Guan and G. Guiochon, J. Chromatogr. A, 731 (1996) 27.
[12] C.J. Dunlap and P.W. Carr, J. Chromatogr. A, 746 (1996) 199.
[13] S. Brunauer, P.H. Emmett and E. Teller, J. Am. Chem. Soc., 60 (1938) 309.
[14] E.P. Barrett, L.G. Joyner and P.P. Halenda, J. Am. Chem. Soc., 73 (1951) 373.
[15] E. Cassasa, J. Polym. Sci., B5 (1967) 773.
[16] L.Z. Vilenchik, J. Asrar, R.C. Ayotte, L. Ternoritsky and C.J. Hardiman, J. Chromatogr., 648 (1993) 9.
[17] H. Guan, G. Guiochon, D. Coffey, E. Davis, K. Gulakowski and D.W. Smith, J. Chromatogr. A, 736 (1996) 21.
[18] G. Guiochon and M.J. Sepaniak, J. Chromatogr., 606 (1992) 248.
[19] M. Sarker, A.M. Katti and G. Guiochon, J. Chromatogr. A, 719 (1996) 275.
[20] R.P. Mayer and R.A. Stowe, J. Coll. Sci., 20 (1965) 893.
[21] B.J. Stanley, C.R. Foster and G. Guiochon, J. Chromatogr. A, 761 (1997) 41.
[22] L. Jelinek and E. sz. Kovats, Langmuir, 10 (1994) 4225.r